Numerical Methods for Separated Flow Solutions around a Circular Cylinder

C. L. Lin,* D. W. Pepper,† and S. C. Lee‡
University of Missouri-Rolla, Rolla, Mo.

Numerical solutions of the Navier-Stokes equations were obtained for separated flows around a circular cylinder at Reynolds numbers 40, 80, and 200. The flowfields were obtained by using three finite-difference techniques. The implicit scheme solved by matrix factorizations gave the best accuracy and used the least computer time. The flow pattern in the recirculating region of a circular cylinder begins to oscillate as the Reynolds number exceeds 40. The calculated drag coefficients, separation angles, and Strouhal numbers were compared with available experimental data. Computational inaccuracy resulting from numerical approximations needs to be identified before a complicated flow phenomenon can be realistically analyzed.

Nomenclature

a = arbitrary constant for coordinate transformation
f = frequency of Kármán vortex street
$[L]$ = lower matrix after modification
$[M]$ = coefficient matrix
m = number of iterations
$[N]$ = modifier of the coefficient matrix
n = number of time-steps
$\{q\}$ = column matrix
r = radial coordinate
R = radius of the cylinder
Re = Reynolds number, $2UR/\upsilon$
S = Strouhal number, $2fR/U$
t = time
$[U]$ = upper matrix after modification
U = freestream velocity
V_θ = velocity in the θ direction
V_r = velocity in the r direction
Z = nondimensionalized radial coordinate
ω = vorticity
ψ = stream function
υ = kinematic viscosity
θ = angular coordinate
Δt = time increment
$\Delta\theta$ = angular increment
ΔZ = radial increment
$\{\Phi\}$ = column matrix

I. Introduction

BECAUSE the Navier-Stokes equations are nonlinear, exact solutions are not currently available. The necessity of providing reasonable estimates for complicated flow phenomena leaves research engineers very little choice. The numerical method is one of the very few acceptable tools that is capable of making any contribution to engineering designs or environmental controls. Recent developments in high-speed digital computers make this approach both effective and popular; however, every numerical approach for a given physical problem requires both physical assumptions and mathematical approximations. Computer solutions, especially in practical problems of questionable physical assumptions such as an unverified closure scheme for turbulent flows as discussed by Lee and Harsha[1] and Pepper and Lee,[2] may appear to give reasonable results by substituting unrealistic physical assumptions with incorrect mathematical approximations. One needs to test a numerical method for its accuracy in the developing stage by applying it to a given problem that requires no physical assumptions. Separated flow around a circular cylinder at relatively low Reynolds numbers is one of the thoroughly investigated problems that can provide the basis for such a study in numerical accuracy.

Numerical techniques for solving partial differential equations have been discussed by Conte,[3] Richtmyer,[4] Roache,[5] and many others. Solutions for separated flow problems usually require substantial computer time because of the elliptical nature of the governing equations. Multidimensional separated flows occur in many engineering and environmental problems, which require not only the solution of the Navier-Stokes equations but also the simultaneous solutions of the energy and species equations. Past experience indicates that some numerical techniques may give better accuracy, whereas others may need less computer time. To avoid an unnecessary waste of effort and resources, we conducted a preliminary investigation in which we applied several commonly used numerical methods to a thoroughly investigated problem for the purpose of comparing the numerical accuracy and the required computer time.

The problem of separated flow around a circular cylinder has been thoroughly investigated both experimentally and theoretically. Available information on drag coefficients, separation angles, and Strouhal numbers has been reported by Schlichting,[6] Thoman and Szewczyk,[7] and many others. In the present study, physical evidence will be used for investigating the effect of numerical approximations on solutions of elliptical partial differential equations.

II. Analysis

The governing equations for an incompressible, two-dimensional, unsteady laminar flow over a circular cylinder can be written as

$$\frac{\partial\omega}{\partial t}+\frac{1}{r}\frac{\partial(r\omega V_r)}{\partial r}+\frac{1}{r}\frac{\partial(\omega V_\theta)}{\partial\theta}=\upsilon\left[\frac{1}{r}\frac{\partial}{\partial r}\left(r\frac{\partial\omega}{\partial r}\right)+\frac{1}{r^2}\frac{\partial^2\omega}{\partial\theta^2}\right] \tag{1}$$

with

$$\omega=\frac{1}{r}\left[\frac{\partial(rV_\theta)}{\partial r}-\frac{\partial V_r}{\partial\theta}\right] \tag{2}$$

Presented at the AIAA 2nd Computational Fluid Dynamics Conference, Hartford, Conn., June 19-20 (no preprints, pp. 91-100 bound volume conference papers); submitted June 20, 1975; revision received March 8, 1976. This research was partially supported by the Office of Naval Research contract N00014-75-C-0180.

Index categories: Viscous Nonboundary-Layer Flows; Computer Technology and Computer Simulation Techniques.

*Research Associate, Department of Mechanical and Aerospace Engineering and Graduate Center for Cloud Physics Research.

†Postdoctoral Fellow; presently Research Meteorologist, E. I. du Pont de Nemours, Savannah River, Aiken, S. C.

‡Professor, Department of Mechanical and Aerospace Engineering. Member AIAA.

In these equations, ω is the vorticity, and V_r and V_θ are the velocity components in the r and θ directions, respectively. In terms of the stream function ψ the velocity components may be written as

$$V_r=[(1/r)(\partial\psi/\partial\theta)], \quad V_\theta=\partial\psi/\partial r \tag{3}$$

When radius R is used as the characteristic length and the freestream velocity U as the characteristic velocity, the nondimensionalized stream function and vorticity become

$$\psi'=\psi/UR, \quad \omega'=\omega R/U \tag{4}$$

The independent variables of t, r, and θ are

$$t'=tU/R, \quad r'=r/R, \quad \theta'=\theta/\mathrm{a} \tag{5}$$

in which a is an arbitrary constant for controlling the increment of the transformed coordinate. Because the flowfield variations take place more rapidly in the vicinity of the cylinder than in regions at large distances from the cylinder, it is convenient to transform the radial coordinate by an exponential function,

$$e^{aZ}=r/R \tag{6}$$

The nondimensionalized governing equations with the primes eliminated for simplicity then become:

$$\mathrm{a}^2e^{2aZ}\frac{\partial\omega}{\partial t}-\frac{\partial\psi}{\partial\theta}\frac{\partial\omega}{\partial Z}+\frac{\partial\psi}{\partial Z}\frac{\partial\omega}{\partial\theta}=\frac{2}{Re}\left[\frac{\partial^2\omega}{\partial Z^2}+\frac{\partial^2\omega}{\partial\theta^2}\right] \tag{7}$$

and

$$\omega=\frac{1}{\mathrm{a}^2e^{2aZ}}\left[\frac{\partial^2\psi}{\partial Z^2}+\frac{\partial^2\psi}{\partial\theta^2}\right] \tag{8}$$

in which Re is the Reynolds number based on the diameter of the circular cylinder and the freestream velocity.

III. Finite-Difference Methods

Numerical solutions were obtained by writing the governing differential equations of vorticity, Eq. (7), and stream function, Eq. (8), into finite difference forms. By using i and j to denote the locations in the θ and Z directions, respectively, and employing m for the number of iterations and n for the number of time-steps, numerical solutions for the separated flow around a circular cylinder were obtained with the following three methods.

A. DDE-GSI

The directional difference explicit (DDE) method, as discussed by Thoman and Szewczyk,[7] was used for solving the vorticity equation. The values of $\omega_{i,j}$ at the $(n+1)$th time-step were calculated by using those of the (n)th time-step through the following relation

$$\begin{aligned}\omega_{i,j}^{n+1}=&\frac{\Delta t}{\mathrm{a}^2e^{2aZ}}\left[1-\frac{4}{Re}\left(\frac{1}{(\Delta Z)^2}+\frac{1}{(\Delta\theta)^2}\right)\right]\omega_{i,j}^n\\&+\frac{2}{Re}\left[\frac{\omega_{i,j+1}^n+\omega_{i,j-1}^n}{(\Delta Z)^2}+\frac{\omega_{i+1,j}^n+\omega_{i-1,j}^n}{(\Delta\theta)^2}\right]\\&+\left[\left(\frac{\partial\psi}{\partial\theta}\omega\right)_{i,j+\frac{1}{2}}^n-\left(\frac{\partial\psi}{\partial\theta}\omega\right)_{i,j-\frac{1}{2}}^n\right]\frac{1}{\Delta Z}\\&-\left[\left(\frac{\partial\psi}{\partial Z}\omega\right)_{i+\frac{1}{2},j}^n-\left(\frac{\partial\psi}{\partial Z}\omega\right)_{i-\frac{1}{2},j}^n\right]\frac{1}{\Delta\theta}\end{aligned} \tag{9}$$

Equation (9) is an explicit form of the nonlinear vorticity equation. In order to maintain numerical stability, the following restrictions were suggested by Thoman and Szewczyk[7] for the nonlinear terms

$$(\partial\psi(\partial\theta)_{i,j+\frac{1}{2}}>0 \qquad \omega_{i,j+\frac{1}{2}}=\omega_{i,j} \tag{10a}$$

$$(\partial\psi/\partial\theta)_{i,j+\frac{1}{2}}<0 \qquad \omega_{i,j+\frac{1}{2}}=\omega_{i,j+1} \tag{10b}$$

$$(\partial\psi/\partial\theta)_{i,j-\frac{1}{2}}>0 \qquad \omega_{i,j-\frac{1}{2}}=\omega_{i,j-1} \tag{10c}$$

$$(\partial\psi/\partial\theta)_{i,j-\frac{1}{2}}<0 \qquad \omega_{i,j-\frac{1}{2}}=\omega_{i,j} \tag{10d}$$

$$(\partial\psi/\partial Z)_{i+\frac{1}{2},j}>0 \qquad \omega_{i+\frac{1}{2},j}=\omega_{i+1,j} \tag{10e}$$

$$(\partial\psi/\partial Z)_{i+\frac{1}{2},j}<0 \qquad \omega_{i+\frac{1}{2},j}=\omega_{i,j} \tag{10f}$$

$$(\partial\psi/\partial Z)_{i-\frac{1}{2},j}>0 \qquad \omega_{i-\frac{1}{2},j}=\omega_{i,j} \tag{10g}$$

$$(\partial\psi/\partial Z)_{i-\frac{1}{2},j}<0 \qquad \omega_{i-\frac{1}{2},j}=\omega_{i-1,j} \tag{10h}$$

Once the vorticity values were obtained, the stream functions could be calculated by using the Gauss-Seidel iteration (GSI) method as discussed by Conte.[3] The values of $\psi_{i,j}$ at the $(n+1)$th time-step and the $(m+1)$th iteration were calculated by using the following relation

$$\begin{aligned}\psi_{i,j}^{m+1}=&\frac{1}{d_{i,j}}\left[-\mathrm{a}^2e^{2aZ}\omega_{i,j}^n+\frac{1}{(\Delta Z)^2}\left(\psi_{i,j+1}^m+\psi_{i,j-1}^{m+1}\right)\right.\\&\left.+\frac{1}{(\Delta\theta)^2}\left(\psi_{i+1,j}^m+\psi_{i-1,j}^{m+1}\right)\right]\end{aligned} \tag{11}$$

in which $d_{i,j}=[2/(\Delta Z)^2]+[2/(\Delta\theta)^2]$. The iteration process was completed when the difference of the numerical values of ψ between the $(m+1)$th and the (m)th iterations was less than a prescribed tolerance. The same procedure was repeated for the successive time-steps until steady-state solutions were reached.

B. ADI-SOR

The alternating directional implicit (ADI) method was proposed by Peaceman and Rachford[8] for solving linear differential equations and modified by Douglas,[9] Wachspress,[10] and many others for improving computational accuracy. Son and Hanratty[11] used the method for flow around circular cylinders with the assumption that the flowfield is symmetric to the axis of the flow direction. Lin and Lee[12] used the method for calculating transient flows around a sphere. However, it was noted that for most Reynolds numbers separated flow oscillates in the wake region. By eliminating the assumption of flow symmetry in the wake region, an extension of Lin and Lee's approach was used for solving the vorticity equation. Two half-time steps were used. The first half-time step is an implicit finite difference equation in the θ direction

$$T_{i+1,j}\omega_{i+1,j}^{n+\frac{1}{2}}+T_{i,j}\omega_{i,j}^{n+\frac{1}{2}}+T_{i-1,j}\omega_{i-1,j}^{n+\frac{1}{2}}=T \tag{12}$$

in which

$$T_{i+1,j}=\frac{1}{4\Delta Z\Delta\theta}(\psi_{i,j+1}^n-\psi_{i,j-1}^n)-\frac{2}{Re(\Delta\theta)^2} \tag{13a}$$

$$T_{i,j}=\frac{2\mathrm{a}^2e^{2aZ}}{\Delta t}+\frac{4}{Re(\Delta\theta)^2} \tag{13b}$$

$$T_{i-1,j}=-\frac{1}{4\Delta Z\Delta\theta}(\psi_{i,j+1}^n-\psi_{i,j-1}^n)-\frac{2}{Re(\Delta\theta)^2} \tag{13c}$$

and

$$\begin{aligned}T=&\left[\frac{1}{4\Delta Z\Delta\theta}(\psi_{i+1,j}^n-\psi_{i-1,j}^n)+\frac{2}{Re(\Delta Z)^2}\right]\omega_{i,j+1}^n\\&+\left[\frac{2\mathrm{a}^2e^{2aZ}}{\Delta t}-\frac{4}{Re(\Delta Z)^2}\right]\omega_{i,j}^n+\left[\frac{2}{Re(\Delta Z)^2}\right.\\&\left.-\frac{1}{4\Delta Z\Delta\theta}(\psi_{i+1,j}^n-\psi_{i-1,j}^n)\right]\omega_{i,j-1}^n\end{aligned} \tag{13d}$$

The second half-time step is an implicit finite-difference equation in the Z direction

$$S_{i,j+1}\omega_{i,j+1}^{n+1}+S_{i,j}^{n+1}\omega_{i,j}+S_{i,j-1}^{n+1}\omega_{i,j-1}=S \tag{14}$$

in which

$$S_{i,j+1}=-\frac{1}{4\Delta Z\Delta\theta}(\psi_{i+1,j}^{n}-\psi_{i-1,j}^{n})-\frac{2}{Re(\Delta Z)^2} \tag{15a}$$

$$S_{i,j}=\frac{2a^2e^{2aZ}}{\Delta t}+\frac{2}{Re(\Delta Z)^2} \tag{15b}$$

$$S_{i,j-1}=\frac{1}{4\Delta Z\Delta\theta}(\psi_{i+1,j}^{n}-\psi_{i-1,j}^{n})-\frac{2}{Re(\Delta Z)^2} \tag{15c}$$

and

$$S=\left[\frac{1}{4\Delta Z\Delta\theta}(\psi_{i,j+1}^{n}-\psi_{i,j-1}^{n})+\frac{2}{Re(\Delta\theta)^2}\right]\omega_{i+1,j}^{n+1/2}+\left[\frac{2a^2e^{2aZ}}{\Delta t}-\frac{4}{Re(\Delta\theta)^2}\right]\omega_{i+1,j}^{n+1/2}+\left[\frac{\psi_{i,j+1}^{n}-\psi_{i,j-1}^{n}}{4\Delta Z\Delta\theta}+\frac{2}{Re(\Delta\theta)^2}\right]\omega_{i-1,j}^{n+1/2} \tag{15d}$$

Solutions of $\omega_{i,j}$ at the $(n+1)$th time-step were used in a successive over-relaxation (SOR) method for calculating the stream functions by the following relation

$$\psi_{i,j}^{m+1}=\psi_{i,j}^{m}+\frac{\lambda}{S'_{i,j}}[a^2e^{2aZ}\omega_{i,j}^{n+1}-S'_{i,j-1}\psi_{i,j-1}^{m+1}-S'_{i-1,j}\psi_{i-1,j}^{m+1}-S'_{i,j}\psi_{i,j}^{m}-S'_{i+1,j}\psi_{i+1,j}^{m}-S'_{i,j+1}\psi_{i,j+1}^{m}] \tag{16}$$

in which

$$S'_{i,j-1}=\frac{1}{(\Delta Z)^2},\quad S'_{i+1,j}=\frac{1}{(\Delta\theta)^2},\quad S'_{i,j}=-\frac{2}{(\Delta Z)^2}-\frac{2}{(\Delta\theta)^2},$$

$$S'_{i+1,j}=S_{i-1,j},\quad S'_{i,j+1}=S'_{i,j-1} \tag{17a-e}$$

The term λ indicates the optimum relaxation factor. The value of λ, which equals 1.65, was used in the analysis based on the method given by Carre.[13] The stream functions $\psi_{i,j}$ at the $(n+1)$th time step were obtained when the difference between the $(m+1)$th iteration and the (m)th iteration was within a prescribed tolerance. The same procedures were repeated for the successive time-steps until the steady state was reached.

C. SIP-SIP

The strongly implicit procedure (SIP) was proposed by Stone[14] for solving linear elliptical partial differential equations. Solutions of vorticity and stream function were obtained separately at each time-step. The vorticity values at the $(n+1)$ time-step were calculated by using the following finite difference equation

$$B_{i,j}\omega_{i,j-1}^{n+1}+D_{i,j}\omega_{i-1,j}^{n+1}+E_{i,j}\omega_{i,j}^{n+1}+F_{i,j}\omega_{i+1,j}^{n+1}+H_{i,j}\omega_{i,j+1}^{n+1}=q_{i,j} \tag{18}$$

in which

$$B_{i,j}=\frac{\psi_{i+1,j}^{n}-\psi_{i-1,j}^{n}}{4\Delta Z\Delta\theta}-\frac{2}{Re(\Delta Z)^2} \tag{19a}$$

$$D_{i,j}=-\frac{\psi_{i,j+1}^{n}-\psi_{i,j-1}^{n}}{4\Delta Z\Delta\theta}-\frac{2}{Re(\Delta\theta)^2} \tag{19b}$$

$$E_{i,j}=\frac{4}{Re}\left[\frac{1}{(\Delta Z)^2}+\frac{1}{(\Delta\theta)^2}\right]+\frac{a^2e^{2aZ}}{\Delta t} \tag{19c}$$

$$F_{i,j}=\frac{\psi_{i,j+1}^{n}-\psi_{i,j-1}^{n}}{4\Delta Z\Delta\theta}-\frac{2}{Re(\Delta\theta)^2} \tag{19d}$$

$$H_{i,j}=-\frac{\psi_{i+1,j}^{n}-\psi_{i-1,j}^{n}}{4\Delta Z\Delta\theta}-\frac{2}{Re(\Delta Z)^2} \tag{19e}$$

$$q_{i,j}=\frac{a^2e^{2aZ}\omega_{i,j}^{n}}{\Delta t} \tag{19f}$$

The SIP method uses a technique of matrix factorization and elimination, as discussed by Stone[14] and Weinstein et al.[15] Detailed procedures are given in the Appendix. The values of stream function were obtained by the same SIP method through the application of the following finite-difference equation

$$B'_{i,j}\psi_{i,j-1}^{n+1}+D'_{i,j}\psi_{i-1,j}^{n+1}+E'_{i,j}\psi_{i,j}^{n+1}+F'_{i,j}\psi_{i+1,j}^{n+1}+H'_{i,j}\psi_{i,j+1}^{n+1}=q'_{i,j} \tag{20}$$

in which

$$B'_{i,j}=\frac{1}{(\Delta Z)^2},\quad D'_{i,j}=\frac{1}{(\Delta\theta)^2},\quad E'_{i,j}=-\frac{2}{(\Delta Z)^2}-\frac{2}{(\Delta\theta)^2},$$

$$F'_{i,j}=D'_{i,j},\quad H'_{i,j}=B'_{i,j},\quad q'_{i,j}=a^2e^{2aZ}\omega_{i,j}^{n+1} \tag{21a-f}$$

Theoretically, the SIP-SIP method could be used directly for steady-state solutions if the boundary conditions were known. Our problem was that the vorticity values at the surface of the cylinder could not be prescribed. Moreover, we were interested in investigating the oscillation phenomenon in the wake region. Consequently, vorticity solutions of successive time-steps were necessary.

IV. Boundary Conditions

Based on no-slip conditions, the velocity components are zero at the surface of the cylinder, whereas a uniform flowfield of velocity U surrounds the cylinder. The boundary conditions for the stream functions and vorticities in terms of the transformed coordinates (Z,θ) are given in Fig. 1. It is noted that the vorticity values at the cylinder surface can only be determined from the second derivatives of the local stream functions by the relation

$$\omega=\left[\frac{1}{a^2e^{2aZ}}\frac{\partial^2\psi}{\partial Z^2}\right]_{Z=0}\quad\text{for all }\theta \tag{22}$$

In finite-difference form at $Z=0$, the vorticity values for all θ become

$$\omega_{i,j}=[\psi_{i,j+1}-2\psi_{i,j}+\psi_{i,j-1}]/a^2(\Delta Z)^2 \tag{23}$$

On the surface of the cylinder, $Z=0$, the stream function is zero, $\psi_{i,j}=0$. The stream function inside the cylinder, $\psi_{i,j-1}$, is assumed to be the mirror image of the stream function around the cylinder, $\psi_{i,j+1}$, because of zero gradient. Consequently, the values of $\omega_{i,j}$ on the surface for all θ can be written as

$$\omega_{i,j}=2\psi_{i,j+1}/a^2(\Delta Z)^2 \tag{24}$$

The values of $\psi_{i,j+1}$, which are not known at steady state, can, in an iteration process, be arbitrarily assumed to determine the steady-state condition. The number of iterations, if they converge, may depend on the initial assumptions that require some criteria in order to have any consistency. Because we were interested in finding steady-state solution for both

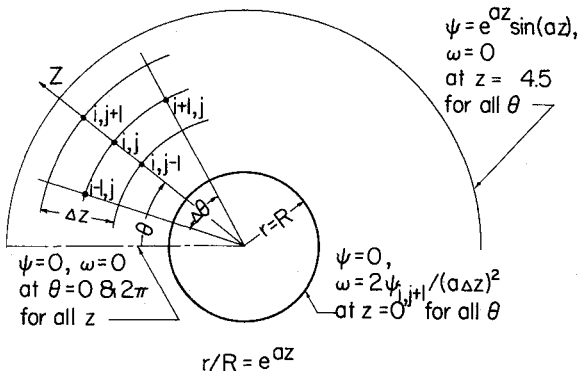

Fig. 1 Boundary conditions.

oscillating and nonoscillating flows, it was to our advantage to use the impulsively started flow as the initial condition. The number of time-steps (NT) indicates the history of flow oscillations. Because the oscillation phenomenon is a part of two-dimensional separated flows, steady state is defined by the following conditions: 1) For nonoscillating flows, the values of ψ and ω remain constant at a given Z and θ location as NT increases; 2) For oscillating flows, the variations of ψ and ω in the Z and θ plane repeat themselves with a definite pattern as NT increases. Numerical solutions for separated flow around a circular cylinder were calculated at three Reynolds numbers (40, 80, and 200) by using three different numerical methods.

V. Results and Discussion

The effect of mesh sizes and outer boundary locations on numerical accuracy has been discussed by Lin and Lee[12] for solutions of Navier-Stokes equations. The current study was undertaken to investigate the relative accuracy and computer time of three different methods. Only one standard mesh size of $\Delta Z=0.1$, $\Delta\theta=6°$, and $\Delta t=0.02$ was used for a flowfield with an outer boundary of 90 radii of the cylinder. To determine the relative accuracy of each method, calculated results of drag coefficient, separation angle, and Strouhal number were compared with available experiemental data. It was found that the SIP-SIP method gave the same accuracy as the ADI-SOR method, which proved better accuracy than the DDE-GSI method. The required computer time on an IBM 370-168 computer is shown in Table 1. It is evident that the SIP-SIP method is a more efficient method for the investigated problem. In order to provide a complete picture of the investigated result, the discussion is divided into two parts.

A. Flow Patterns

The stream function pattern calculated from the SIP-SIP method is shown in Fig. 2 for the case of Reynolds number 40. It is noted that the separated flow in the wake of a circular cylinder is symmetric and steady as long as the Reynolds number is less than 40. The wake length is two to three times as great as the cylinder diameter, and the separation angle is about 126° from the leading edge. Figure 3 shows that streamline pattern for the case of Reynolds number 80. The separation angle is about 114°. The recirculating flow in the wake region oscillates with a definite frequency. The flow pattern appears to repeat itself between 2500 NT and 3150 NT. By using the dimensionless time increment $\Delta t=0.02$, the

Table 1 Computer time comparisons

	IBM 370-168		
Re/Time (min)	DDE-GSI	ADI-SOR	SIP-SIP
40	100	100	40
80	120	120	50
200	–	–	60

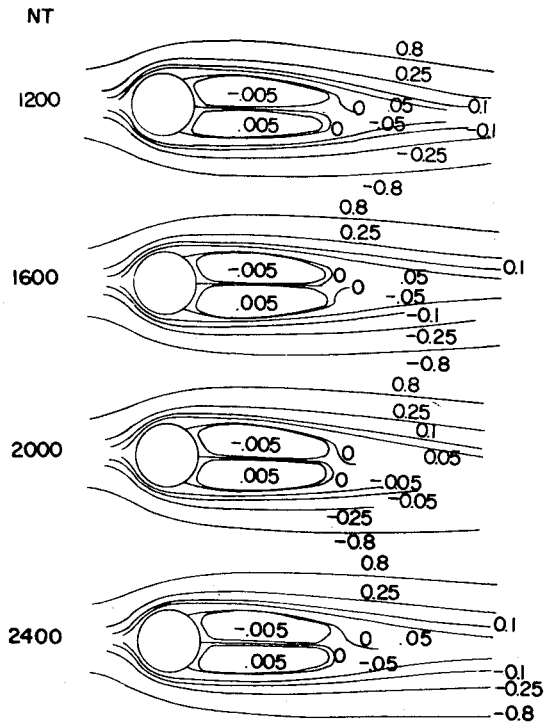

Fig. 2 Streamline patterns, $Re=40$.

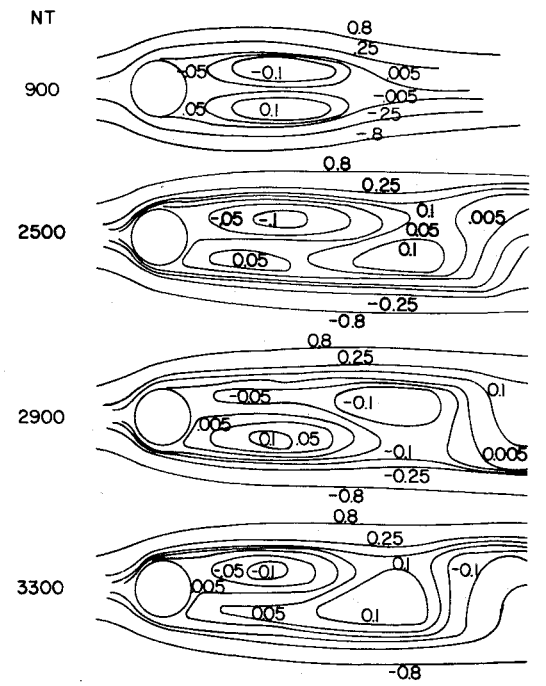

Fig. 3 Streamline patterns, $Re=80$.

oscillating frequency can be calculated by the following equation

$$f=U/R\Delta t[(\mathrm{NT})_2-(\mathrm{NT})_1] \tag{25}$$

The Strouhal number, given by the relation

$$S=2Rf/U \tag{26}$$

has a value of 0.154 for the case of Reynolds number 80. Figure 4 shows the streamline pattern for the case of Reynolds number 200. The separation angle is about 102° from the stagnation point of the leading edge. The flow pattern appears to repeat itself between 2400 NT and 2950 NT. This gives a Strouhal number of 0.182 for the case of Reynolds number

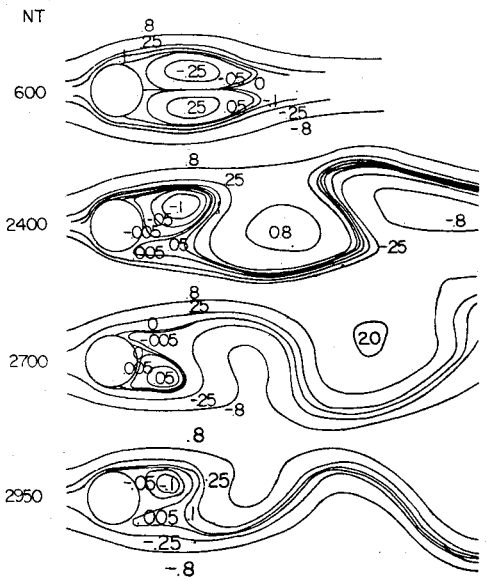

Fig. 4 Streamline patterns.

200. By using the ADI-SOR method, the flow pattern calculations were obtained for cases of Reynolds number 40 and 80 only. The appearances of streamline distributions are very much similar to those of the shown results which were obtained by the SIP-SIP method. The streamline patterns obtained by the DDE-GSI method deviated noticeably from the shown results. In order to answer the question of the relative accuracy of each method, it was necessary to compare the results with available experimental data.

B. Comparison with Experimental Data

Experimental data are available in terms of drag coefficient, separation angle, and Strouhal number. The total drag coefficient is calculated by the summation of the pressure drag coefficient,

$$(C_D)_p = \frac{2}{Re}\int_0^{2\pi}\left\{\int_0^{\infty}\frac{\partial\omega}{\partial\theta}\bigg|_{\theta=0}dZ + \int_0^{\theta}\frac{\partial\omega}{\partial Z}\bigg|_{Z=0}d\theta'\right\}\cos\theta\, d\theta \tag{27}$$

and the skin friction drag coefficient,

$$(C_D)_f = \frac{2}{Re}\int_0^{2\pi}\omega\Big|_{Z=0}\sin\theta d\theta \tag{28}$$

By using the obtained values of vorticity and vorticity gradient along the surface of the cylinder, the drag coefficient for each Reynolds number case was determined and compared with available experimental data.

Numerical solutions were also obtained by other investigators who used one of the three different methods. The DDE-GSI method was used by Thoman and Szewczyk[7] who compared their results with the experimental data of Relf and Simmons as well as with the data of Morkovin. The ADI-SOR method was used by Son and Hanratty who also discussed the numerical results of Kawaguati and Jain. When we used the DDE-GSI method for our calculations in the drag coefficient, we obtained practically the same results as Thoman and Szewczyk; however, when we used the ADI-SOR method for our drag calculations, we got the same results as those obtained by the SIP-SIP method, which is developed in the present work. The assumption that a line of symmetry exists in the wake region appears to be the source of inaccuracy in the numerical results of Son and Hanratty at Reynolds numbers greater than 40. When compared with the experimental data of Perry[16] and Roshko[17] as shown in Fig. 5, this observation was confirmed. It is interesting to note that the discrepancy between experimental data is greater than that of the numerical results at the lower Reynolds number region. The experimental results were also compared with analytical results on separation angles as shown in Fig. 6. The experimental data obtained by Homann[18] at Reynolds number 40 agree well with all analytical results. The DDE-GSI method of Thoman and Szewczyk appears to give the most inaccurate predictions at other Reynolds numbers. This is to be expected, because the criteria given in Eq. (10) for numerical stability tend to generate larger values of inaccuracy in the close vicinity of a solid boundary where the flow separation is originated. Moreover, the assumption of symmetry in the wake region that was used by Son and Hanratty apparently gives reasonable predictions for separation angles because they are located upstream of the wake region. The experimental and numerical results on Strouhal numbers can also be compared as shown in Fig. 7. Because the Strouhal number is related to the shedding of vorticities in the wake region, as given in Eqs. (25) and (26), numerical methods to predict Strouhal numbers cannot assume the line of symmetry in that region. The experimental data of Roshko[17] appear to be consistent at all tested Reynolds numbers. The experimental data of Relf and Simmons as well as the data of Morkovin were used by Thoman and Szewczyk for comparison with their numerical results, which were obtained by the DDE-GSI method. The ADI-SOR method used by Son and Hanratty cannot predict Strouhal numbers, because it assumes symmetry in the wake region. The ADI-SOR method used in the present study gives similar results as the SIP-SIP

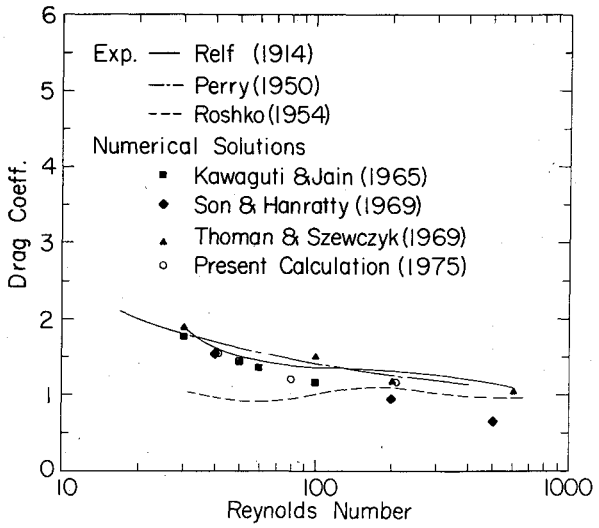

Fig. 5 Drag coefficient comparisons.

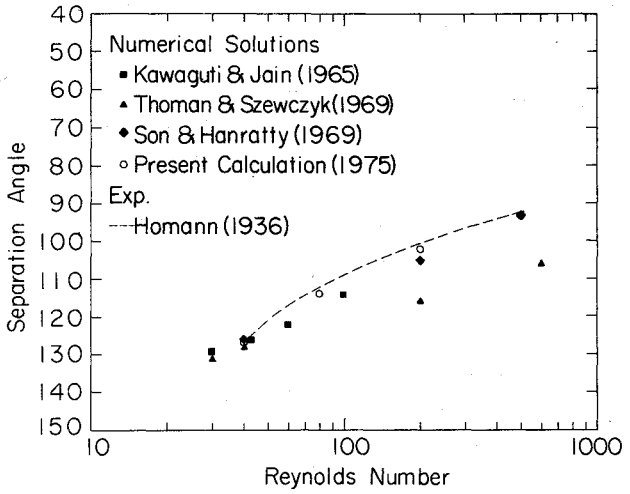

Fig. 6 Separation angle comparisons.

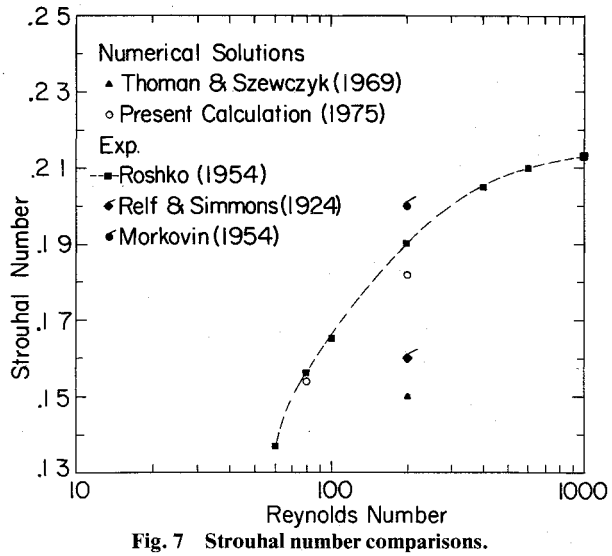

Fig. 7 Strouhal number comparisons.

method for the case of Reynolds number 80 and uses more than twice the amount of computer time than the latter method. Consequently, only the SIP-SIP method has been used for studying the case of Reynolds number 200. It is evident that discrepancies exist in both experimental and numerical results for Strouhal numbers. The present study appears to agree better with Roshko's data than with the data in other studies.

VI. Conclusions

It is necessary to examine a newly developed numerical method for the purpose of correcting questionable mathematical approximations. For solving nonlinear elliptical differential equations, the numerical method which appears to give the best accuracy and uses the least amount of computer time is the implicit finite difference scheme that is solved by matrix factorizations.

Separated flow around a circular cylinder can have a line of symmetry in the wake region only at Reynolds numbers less than 40. In the case of oscillating flows, there are two factors which cause errors in numerical solutions. One is the mathematical approximation of the nonlinear terms that is used to achieve numerical stability. The other is the physical assumption of the wake symmetry. Calculations of the drag coefficient appear to be within the limit of experimental accuracy if the physical reality of flow oscillations is allowed in the wake region. Calculations of the separation angle appear to be affected more significantly by the mathematical approximation than the physical assumption. Calculations of the Strouhal number, however, require an adequate treatment of both factors.

The question on computer simulations vs wind-tunnel simulations can only be answered according to the purpose of applications.

1) For laminar flows at relatively low Reynolds numbers, it is economically advantageous to use computer simulations because the technology available today is adequate.

2) As the Reynolds numbers increase to the region of instability, computer simulations using unsteady-state Navier-Stokes equations are questionable, because the numerical instability is not distinguishable from flow instability. However, wind-tunnel simulations may have the same problem of super-positioning mechanical vibrations upon flow instabilities.

3) In the turbulent flow region, computer simulations need to use time-steps at least one order of magnitude smaller than the smallest period of the turbulent fluctuation. This will enable us to solve the unsteady-state Navier-Stokes equations by considering the fluctuating velocities as time dependent variables of the momentary velocity components. However, today's computer technology cannot reach the required computational speed. Computer simulations of turbulent flow problems are presently being conducted by using a closure scheme to relate the turbulent fluctuations with the time-averaged components. Owing to the limited availability of reliable experimental data, there is a possibility of super-positioning questionable mathematical approximations upon unrealistic physical assumptions. This is particularly true when the solution of nonlinear elliptical partial differential equations is required for turbulent flows in the separation region. The present study is intended to minimize the numerical inaccuracy before a closure scheme is introduced into turbulent flow problems. Consequently, computer and wind-tunnel simulations are both necessary to improve our current understanding of turbulent flows.

4) Turbulent flows with heat, mass, and momentum transfer often simultaneously occur in many practical problems, such as combustion engineering, environmental pollution, and weather prediction. A realistic computer simulation technique will require the advanced technology in both computational speed and computer storage which are yet to be developed to the operational stage. In the foreseeable future, wind-tunnel simulation is considered to be the most reliable method before full-scale testing for any successful engineering design can be realized. However, the economical reality in conducting extensive experimental investigations makes it necessary for computer simulations of approximate nature to be used to supplement both wind-tunnel simulations and full-scale testing. For practical purposes, both computers and wind tunnels are necessary to supplement each other to provide the reliablity and economy that are required for all successful engineering endeavors.

Table 2 Elements of matrices $[M]$, $\{\Phi\}$, and $\{q\}$ [a]

$$[M] \qquad \{\phi^{n+1}\} = \{q^n\}$$

$$\begin{bmatrix} E_{1,1} & F_{1,1} & H_{1,1} & & & \\ D_{2,1} & E_{2,1} & F_{2,1} & H_{2,1} & & \\ & D_{1,1} & E_{1,1} & F_{1,1} & H_{1,1} & \\ B_{1,2} & & D_{1,2} & E_{1,2} & F_{1,2} & H_{1,2} \\ & B_{i,j} & & D_{i,j} & E_{i,j} & F_{i,j} & H_{i,j} \\ & & B_{I,J} & & D_{I,J} & E_{I,J} \end{bmatrix} \begin{Bmatrix} \phi_{1,1} \\ \phi_{2,1} \\ \phi_{1,1} \\ \phi_{1,2} \\ \phi_{i,j} \\ \phi_{I,J} \end{Bmatrix} = \begin{Bmatrix} q_{1,1} \\ q_{2,1} \\ q_{1,1} \\ q_{1,2} \\ q_{i,j} \\ q_{I,J} \end{Bmatrix}$$

[a] I is the maximum number of points in the i direction; J is the maximum number of points in the j direction.

Appendix

Using the SIP Method to Obtain the Matrix Solution

The governing equations, in matrix form, with five nonzero diagonal elements as the coefficient matrix may be written for either Eq. (18) or Eq. (20) as follows

$$[M]\cdot\{\Phi^{n+1}\}=\{q^n\} \tag{A1}$$

The term $[M]$ is the coefficient matrix of the column matrix $\{\Phi^{n+1}\}$, which represents either the stream function ψ or the vorticity ω at the $(n+1)$th time-step for every grid point in the flowfield. The column matrix $\{q^n\}$ results from the known values of the flowfield at the (n)th time-step. The elements of matrices $[M]$, $\{\Phi\}$, and $\{q\}$ are given in Table 2. In order to accelerate the solution procedure, matrix $[M]$ is modified as matrix $[M+N]$, which consists of seven nonzero diagonal elements. Equation (A1) then becomes

$$[M+N]\{\Phi^{n+1}\}^{m+1}=\{q^n\}+[N]\{\Phi^{n+1}\}^{m} \tag{A2}$$

in which m is the number of iterations for determining the column matrix $\{\Phi\}$ at the $(n+1)$th time-step. The modifier matrix $[N]$ has to fulfill the requirement that the coefficient matrix $[M+N]$ can be factored into the product of a lower matrix $[L]$ and an upper matrix $[U]$; each consists of three nonzero diagonal elements in the lower and upper portions, respectively, as follows:

$$[M+N]=[L]\,[U] \tag{A3}$$

$$\begin{bmatrix} ① & ② & & & & & \\ & ③ & ④ & ⑤ & & & \\ & & ⑥ & ⑦ & & & \\ & & & & & & \end{bmatrix} = \begin{bmatrix} d_{1,1} & & & & & & \\ c_{2,1} & d_{2,1} & & & & & \\ & b_{1,2} & c_{1,2} & d_{1,2} & & & \\ & & & & & & \\ & & & & & b_{I,J} & c_{I,J}d_{I,J} \end{bmatrix}$$

$$\begin{bmatrix} 1 & e_{1,1} & f_{1,1} & & \\ & 1 & e_{2,1} & f_{2,1} & \\ & & 1 & e_{1,2} & f_{1,2} \\ & & & & \\ & & & & 1 \end{bmatrix} \tag{A4}$$

in which

$$①=b_{i,j}$$

$$②=b_{i,j}e_{i,j-1}$$

$$③=c_{i,j}$$

$$④=d_{i,j}+b_{i,j}f_{i,j-1}+c_{i,j}e_{i-1,j}$$

$$⑤=d_{i,j}e_{i,j}$$

$$⑥=c_{i,j}f_{i-1,j}$$

$$⑦=d_{i,j}f_{i,j}$$

with

$$b_{i,j}=B_{i,j}/(1+\alpha e_{i,j-1})$$

$$c_{i,j}=D_{i,j}/(1+\alpha f_{i-1,j})$$

$$d_{i,j}=E_{i,j}+\alpha(b_{i,j}e_{i,j-1}+c_{i,j}f_{i-1,j})-b_{i,j}f_{i,j-1}-c_{i,j}e_{i-1,j}$$

$$e_{i,j}=(F_{i,j}-\alpha b_{i,j}e_{i,j-1})/d_{i,j}$$

$$f_{i,j}=(H_{i,j}-\alpha c_{i,j}f_{i-1,j})/d_{i,j}$$

The iteration parameter α is allowed to vary between zero and unity. According to Stone[14] values near unity tend to reduce the low-frequency errors more rapidly. In this analysis, ten values of α between zero and unity are evenly distributed in the range between the high and low frequencies.

The purpose of this modification is to determine the column matrix $\{\Phi^{n+1}\}$ by having the difference between the $(m+1)$th and the (m)th iterations within a prescribed tolerance. If a column matrix $\{\Delta\Phi\}$ at the $(m+1)$th iteration is defined as

$$\{\Delta\Phi^{n+1}\}^{m+1}=\{\Phi^{n+1}\}^{m+1}-\{\Phi^{n+1}\}^{m} \tag{A5}$$

then Eq. (A2) can be written as

$$[M+N]\{\Delta\Phi^{n+1}\}^{m+1}=\{q^n\}-[M]\{\Phi^{n+1}\}^{m} \tag{A6}$$

If one uses the lower and upper matrices given by Eq. (A3), Eq. (A6) can be expressed as

$$[L]\,[U]\{\Delta\Phi^{n+1}\}^{m+1}=\{q^n\}-[M]\{\Phi^{n+1}\}^{m} \tag{A7}$$

The use of matrices $[L]$ and $[U]$ accelerates the solution procedures by successive eliminations. Once the column matrix $\{\Delta\Phi^{n+1}\}$ at the $(m+1)$th iteration is equal to or less than the prescribed tolerance, the values of $\{\Phi^{n+1}\}$ at the (m)th iteration become the solutions of either the vorticity or the stream function at the $(n+1)$th time-step.

References

[1] Lee, S. C. and Harsha, P. T., "Use of Turbulent Kinetic Energy in Free Turbulent Mixing Studies," *AIAA Journal*, Vol. 8, June 1970, pp. 1026-1032.

[2] Pepper, D. W. and Lee, S. C., "Transport Phenomena in Thermally Stratified Boundary Layers," *Journal of Heat Transfer*, Vol. 97, Feb. 1975, pp. 60-65.

[3] Conte, S. D., *Elementary Numerical Analysis*, McGraw-Hill, New York, 1965, p. 179.

[4] Richtmyer, R. D., *Difference Methods for Initial-Value Problems*, Interscience Pub., New York, 1957, p. 238.

[5] Roache, P. J., *Computational Fluid Dynamics*, Hermosa Publishers, Albuquerque, N.M. 972, p. 434.

[6] Schlichting, H., *Boundary Layer Theory*, 6th Edition, McGraw-Hill, New York, 1968, p. 747.

[7] Thoman, D. C. and Szewczyk, A. A., "Time-Dependent Viscous Flow Over a Circular Cylinder," *Physics of Fluid Supplement*, Vol. 12, Dec. 1969, pp. 76-86.

[8] Peaceman, D. W. and Rachford, H. H., Jr., "The Numerical Solution of Parabolic and Elliptic Differential Equations," *Journal of the Society of Industrial and Applied Mathematics*, Vol. 3, 1955, pp. 28-41.

[9] Douglas, J., "On the Numerical Integration of $\partial^2U/\partial X^2+\partial^2/\partial Y^2=\partial U/\partial t$ by Implicit Methods," *Journal of the Society of Industrial and Applied Mathematics*, Vol. 3, 1955, pp. 42-65.

[10] Wachspress, E. L., "Optimum Alternating-Direction-Implicit Iteration Parameters for a Model Problem," *Journal of the Society of Industrial and Applied Mathematics*, Vol. 3, 1955, pp. 42-65.

[11] Son, J. S. and Hanratty, T. J., "Numerical Solution for the Flow around a Cylinder at Reynolds Numbers of 40, 200 and 500," *Journal of Fluid Mechanics*, Vol. 35, 1969, pp. 369-386.

[12] Lin, C. L. and Lee, S. C., "Transient State Analysis of Separated Flow around a Sphere," *International Journal of Computer and Fluids*, Vol. 1, 1973, pp. 235-250.

[13] Carre, B. A., "The Determination of the Optimum Accelerating Factor for Successive Over-Relaxation," *Computer Journal*, Vol. 4, 1961, pp. 73-78.

[14]Stone, H. L., "Iterative Solution of Implicit Approximations of Multidimensional Partial Differential Equations," *SIAM Journal of Numerical Analysis*, Vol. 5, 1968, pp. 530-558.

[15]Weinstein, H. G., Stone, H. L., and Kwan, T. V., "Simultaneous Solution of Multiphase Reservoir Flow Equations," *Society of Petroleum Engineers Journal*, 1970, pp. 99-111.

[16]Perry, T., *Chemical Engineering Handbook*, McGraw Hill, New York, 1950, pp. 1017.

[17]Roshko, A., "On the Development of Turbulent Wakes from Vortex Streets," NACA Rept., 1191, 1954.

[18]Homann, F., "Einfluss grosser Zahigkeit bei Stromung um Zylinder," *Forschung Gebiet im Ingenieur Wesens*, Vol. 7, 1936, pp. 1-10.